

# PhotoMultiplier Tubes characterization for the LHCb Calorimeter Upgrade II

Author: Marta Campos Fornés

Facultat de Física, Universitat de Barcelona, Diagonal 645, 08028 Barcelona, Spain.\*

Advisor: Eduardo Picatoste Olloqui

**Abstract:** In the view of the proposed increase in luminosity and the need for more discrete data during LHC Run 5 at CERN, the current detector will be replaced by other systems capable of meeting the new requirements. In this work, we will study the technical characteristics of two different models of PhotoMultiplier Tubes (Hamamatsu R14755U-100 and Hamamatsu R11187) proposed as light sensors of the calorimeter for Upgrade II at the LHCb. We will also address in detail all methodologies of measurement and data analysis applied during their characterization.

## I. INTRODUCTION

The Large Hadron Collider beauty (LHCb) is an experiment at CERN focused on the study of decays in particles containing b and anti-b quarks with the ultimate goal of investigating CP-violation. Unlike other large experiments at CERN, which surround the entire collision point with an enclosed detector, the LHCb uses a series of subdetectors stacked one after another along the beam pipe. In this case, the collision point is close to one of the detector's ends [4].

One of the detector's components is the Electromagnetic Calorimeter (ECAL), employed for measuring the energy of light particles. This calorimeter currently uses *shashlik* technology, which alternates lead plates, responsible for producing showers of secondary particles when hit by particles resulting from decays, and scintillating tiles, which emit an amount of UV light proportional to the energy of the particles entering the calorimeter. After all the energy coming from particles has been transformed into light, it is transmitted through wavelength-shifting fibers to PhotoMultiplier Tubes (PMTs), which are vacuum light sensors that make use of the photoelectric effect to transform that light into a current pulse output signal [1].

The main focus of this work is the characterization of time resolution and gain of two PMTs (Hamamatsu R14755U-100 and Hamamatsu R11187), as well as the study of their viability of implementation for the new ECAL in LHCb Upgrade II.

This upgrade will be implemented during LS4 (Long Shutdown 4), which will start in 2030. All improvements applied during Upgrade II will start operating in LHC Run 5, which aims to function at an instantaneous luminosity up to  $\mathcal{L} = 2 \cdot 10^{34} \text{cm}^{-2} \text{s}^{-1}$  ( $\sim 5 - 10$  times the current luminosity), which implies that the calorimeter must sustain radiation doses up to to  $1 \text{MGy}$  [4].

The proposed increase in luminosity will require the substitution of certain detection modules for designs based on radiation-hard materials. With the goal of re-

ducing aging, in the innermost parts of the calorimeter the *shashlik* technology will be replaced for the *SPACAL* (Spaghetti Calorimeter) structure and the gain of the PMTs used is aimed to be reduced and stay between  $10^3$  and  $4 \cdot 10^3$ , depending on the distance to the beam pipe.

Finally, the decrease in time resolution ( $\sigma_t$ ) of the PMTs, which will mitigate pileup effect, is also contemplated in the main objectives of Upgrade II [9]. The proposed aim is to stay below  $\sigma_t = 20 \text{ps}$ .

This work constitutes a part of ICCUB's R&D programme focused on building a new calorimeter for Upgrade II on the LHCb.

## II. MEASUREMENTS

### A. Experimental set-up

The main function of a PMT is to transform light into a current pulse output proportional to the number of photoelectrons emitted by its photocathode.

A PMT is a device consisting of an input window, where light enters the PMT; a photocathode, where photons excite electrons so that photoelectrons are emitted into the vacuum (photoelectric effect); focusing electrodes; dynode stages, which act as an electron multiplier; and an anode, which functions as the exit point of photoelectrons (see Figure 1).

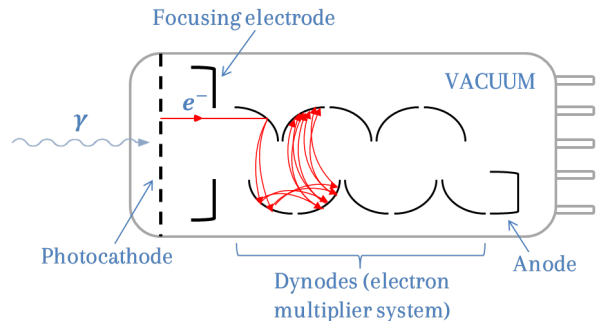


Figure 1: Diagram of the internal structure of a 10-dynode-stage PMT and its functioning.

\*Electronic address: mcampofo7@alumnes.ub.edu

The photoelectron multiplication is a relatively simple process: the photoelectrons emitted by the photocathode are accelerated by an electric field created by the electrical potential difference between the photocathode and the anode, which is generated by a High Voltage supply (HV) connected to the circuit board of the PMT. When the photoelectrons impinge on each dynode, they are multiplied due to secondary electron emission [6].

The technical characteristics of each PMT highly affect their performance. For example, the Hamamatsu R14755U-10 only has 6 dynode stages, whereas the Hamamatsu R11187 has 8, resulting in a higher current amplification.

During this work's experimental phase, two different measurement methods were used: the Single Photoelectron (Single Phe) measurement and the Large Number of Photoelectrons measurement.

In the Single Phe mode of measurement, one assumes that the mean number of photoelectrons (emitted by the photocathode and before multiplication) is less than 1. This is achieved through the placement of an optical beam attenuator in front of the light emission point and can be verified by observing the resulting charge peaks, which will be discussed more in-depth in section II B 2.

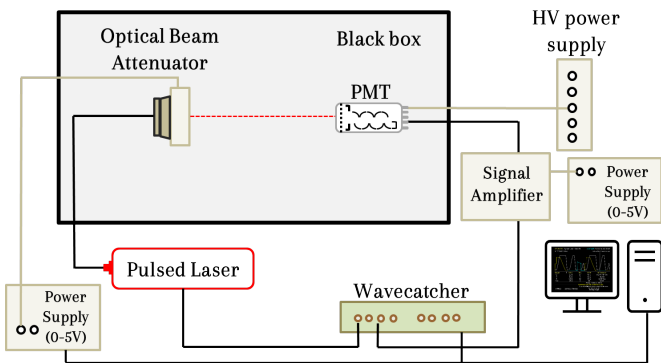


Figure 2: Experimental set-up used during the Single Phe measurements.

The experimental set-up for this type of measurement is illustrated in Figure 2. The red laser source emits pulsed light, which is attenuated by a light filter and later reaches the PMT, the device under test whose circuit board is connected to a High Voltage power supply (HV). The laser source is directly connected to the Wavecatcher, a device that acts like a fast and linear oscilloscope, operates at  $3.5GS/s$ , and is responsible for digitizing both the output signal from the PMT and the input signal for the laser trigger into arrays of 1024 evenly time spaced voltage values. The Wavecatcher is also connected to a  $1200\Omega$  transimpedance amplifier, which amplifies the current pulse output of the PMT and is powered by a Low Voltage power supply (0-5V). The Wavecatcher sends all the information to a computer, which contains a set of Python developed programs that allow us to execute measurements and store, visualize and analyze

data, as well as to control the set-up devices.

As represented in Figure 2, both the laser emitter and the PMT are enclosed in a black box. The motive behind this is that PMTs are extremely sensitive, they can not receive any light coming from the outside.

For the Large Number of Photoelectrons method, the signal amplifier and the optical beam attenuator are removed, but everything else in the set-up is identical.

## B. Experimental methodology and results

This section will describe the different measurement and data analysis methodologies used to obtain time resolution and gain results. Said results will also be presented and analyzed in this same section.

### 1. Time resolution

As previously mentioned, minimizing time resolution in PMTs is crucial for reducing pileup effects.

We define time resolution as the standard deviation of the trigger-to-signal delay histogram created using the 10000 measurements made at each HV value. The basic idea behind this magnitude is to determine the minimum amount of time that must pass between two collisions for the PMT to be able to distinguish them as differentiated signals.

In order to ensure measurement homogeneity regardless of the pulse height, the constant fraction discriminator (CFD) technique [5] was applied.

As a first approximation to the time the trigger was sent out, we always recorded the time index of the voltage component that was closest to 50% of the trigger's voltage amplitude. For the signal emitted by the PMT, the threshold chosen varied: in pursuance of the minimization of time resolution, we used a program that calculated its value for different percentages of voltage amplitude and returned the most optimal one.

The Wavecatcher operates at  $3.5GS/s$ . Therefore, it records data every  $3.125 \cdot 10^{-10}$  s, which is known as its time unit. Since the orders of magnitude of the time unit and the delay were very similar, we applied a secondary method to determine with higher precision the exact time when both the PMT output signal and the trigger reached their established threshold. Considering four consecutive data recordings around the time index we had found on our first approximation, we performed a linear regression (see Figure 3). The choice of using a linear regression was not random, as having also tested the fit of a second-degree polynomial function, we found the former to be the fit that optimized our result. The number of data points chosen to fit the regression also came as a result of a trial-and-error process in which we determined four points to be the number that minimized our time resolution values.

Using this linear regression, we determined new and more precise time values for the exact moments the trigger was sent out and the PMT output signal was detected by the Wavecatcher.

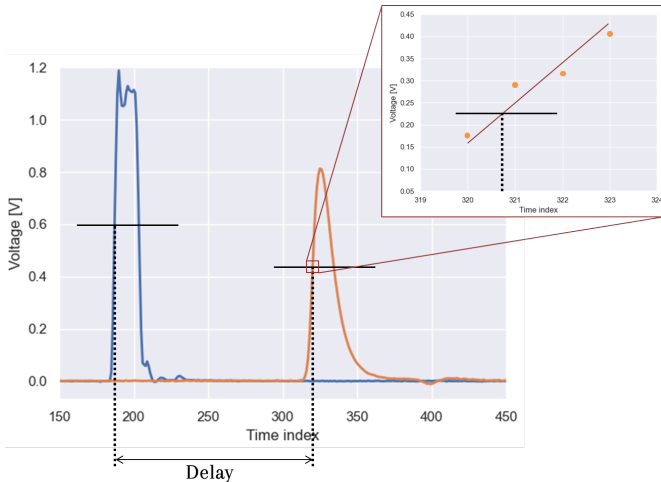


Figure 3: Trigger voltage peak (blue line) and Large Number of Photoelectrons voltage peak (PMT output signal, orange line) corresponding to a measurement taken at  $HV = 450V$  for the Hamamatsu R11187. An example of CFD thresholds has been added for both the trigger and the signal, as well as a linear regression adjusted to the voltage signal curve.

Time resolution values have a strong dependence on both the HV applied to the PMT and the laser intensity, which is why we performed measurements for a wide range of voltage values for both PMTs using the same laser intensity. The HV range used to perform measurements was chosen accordingly to each PMT's optimal working range ( $450V - 750V$  for the Hamamatsu R11187 and  $450V - 1000V$  for the Hamamatsu R14755U-100).

All time resolution results are presented in Figure 4.

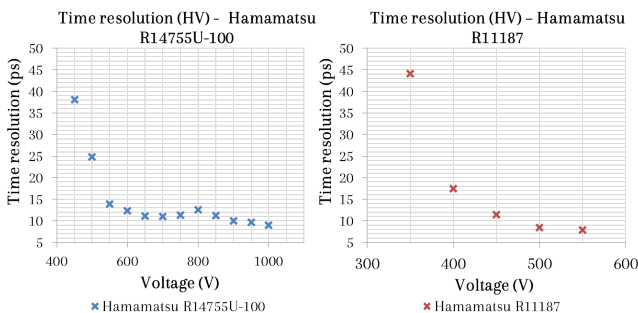


Figure 4: Time resolution values obtained for PMT Hamamatsu R11187 (red crosses) and Hamamatsu R14755U-100 (blue crosses) using the same laser intensity.

Figure 4 shows that for both PMTs, while the HV value increases, the time resolution decreases until it reaches its minimum value, at which point the time resolution remains constant in a *plateau*, regardless of how much

we increase the HV value. Figure 4 shows that, under the circumstances in which we conducted our measurements, the time resolution's minimal value is  $\sigma_t \approx 9ps$  for the Hamamatsu R14755U-100 (reached at almost  $HV = 1000V$ ) and  $\sigma_t \approx 8ps$  for the Hamamatsu R11187 (reached at approximately  $HV = 550V$ ).

Therefore, we can assume that the Hamamatsu R11187 has slightly lower time resolution values for the same working conditions, but the difference isn't substantial enough to determine if any of the PMTs has a greater viability of implementation at LHCb's calorimeter than the other.

## 2. Gain

The gain ( $G$ ) of a PMT, also known as its current amplification, changes in relation to the supply voltage as follows [6]:

$$G = G_0 \cdot V^\alpha \quad (1)$$

Where  $G_0$  and  $\alpha$  are characteristic constants for each PMT model.

The recording of each measurement returned a voltage peak akin to the one plotted in orange in Figure 3. In order to calculate the current amplification, we integrated the voltage peak with respect to time for each of the 10000 measurements using the trapezoid method, we created a histogram using these results, we identified the most common charge value by fitting the histogram, and we divided the obtained charge value by  $e$ , an electron's charge.

The histogram of 10000 charge values obtained using Single Phe measurements had two peaks. One is the pedestal charge value (originated from events with no light on the PMT and centered around null charge) and the other one is the Single Photoelectron charge peak, the latter being the one we are mostly interested in.

When it came to fitting the histogram created using the Single Phe measurements, we used two different models: a double gaussian fit and the Bellamy function fit [2] (see Equation IIB 2 and Figure 5). Both fits were performed using Python programs. In the particular case of the Bellamy function, due to the large number of parameters that needed to be determined, we developed a code using ROOT libraries from CERN.

The Bellamy function has the following algebraic expression [2] and takes into account all PMT internal processes:

$$f(x) = A \sum_{n=0}^{\infty} \frac{\mu^n e^{-\mu}}{n!} \left\{ (1-w) \cdot G_n(x, \sigma_n) + w \frac{\alpha}{2} \cdot e^{-\alpha(x-Q_n-\alpha\sigma_n^2)} \left[ erf \left( \frac{|Q_0 - Q_n - \alpha\sigma_n^2|}{\sigma_n \sqrt{2}} \right) + \right. \right. \quad (2)$$

$$\left. \left. + sign(x - Q_n - \alpha\sigma_n^2) \cdot erf \left( \frac{|x - Q_n - \alpha\sigma_n^2|}{\sigma_n \sqrt{2}} \right) \right] \right\}$$

Where:

$$G_n(x, \sigma_n) = \frac{N_n}{\sigma_n \sqrt{2\pi}} \cdot e^{-\frac{(x-Q_n)^2}{2\sigma_n^2}}$$

$$N_n = \begin{cases} A_0 & \text{if } n = 0 \\ 1 & \text{if } n > 0 \end{cases} \quad Q_n = Q_0 + nQ_1$$

$$\sigma_n = \sqrt{\sigma_0^2 + n\sigma_1^2} \approx \begin{cases} \sigma_0 & \text{if } n = 0 \\ \sqrt{n}\sigma_1 & \text{if } n > 0 \end{cases}$$

$A$  and  $A_0$  are normalization constants,  $w$  is the probability that a measured signal is accompanied by a discrete background process,  $\alpha$  is the coefficient of exponential decrease of the background processes described by  $w$ ,  $Q_0$  and  $Q_1$  are the charges of the pedestal and Single Phe voltage peak,  $\sigma_0$  and  $\sigma_1$  are the respective standard deviations for the pedestal and the Single Phe charge distributions,  $erf$  is the error function and  $sign$  is the sign function.

The parameter  $\mu$  is the mean number of photoelectrons collected by the first dynode of the PMT and is defined as  $\mu = mq$ , where  $m$  is the mean number of photons hitting the photocathode and  $q$  is the quantum efficiency of the photocathode, which is the ratio between the emitted photoelectrons and the impinging photons.

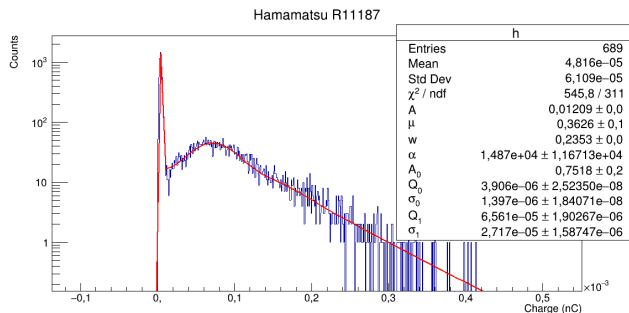


Figure 5: Charge(nC) histogram of a Single Phe measurement for the Hamamatsu R11187 PMT at  $HV = 750V$  fitted using the Bellamy function.

As mentioned above, gain values can also be obtained using Large Number of Photoelectrons measurements. In this case, a new concept must be taken into account: the number of photoelectrons ( $N_{phe}$ ) emitted by the photocathode [3]:

$$N_{phe} = \left( \frac{Q_n - Q_0}{\sigma_n} \right)^2, \quad G = \frac{Q_n}{e \cdot N_{phe}} \quad (3)$$

Where  $Q_n$  and  $\sigma_n$  are the charge value associated to the Large Number of Photoelectrons voltage peak and the standard deviation of the charge value distribution, which are identified through the fitting of a double gaussian model (see Appendix A).

Both methods of measurement and data analysis presented above were designed for PMTs with a high

signal-to-noise ratio. However, that is not necessarily the case for PMT Hamamatsu R14755U-100, as noise voltage values are comparable to signal peak values, especially for the Single Phe measurements.

Taking this into consideration, the choice of laser intensity for Single Phe measurements was key, a balance needed to be achieved: maximizing the laser intensity without saturating the Wavecatcher.

For Large Number of Photoelectrons measurements, the low signal-to-noise ratio mostly affected the relation between gain and voltage expressed in Equation 1, which is why the *Excess Noise Factor* ( $F$ ) was taken into account, a factor that considers the noise contributions from the PMT multiplier chain of dynodes.  $F$ , assuming an equally-distributed divider, is defined as [3]:

$$F = \frac{1}{\delta - 1} \left( 1 - \frac{1}{\delta^d} \right) = \frac{1}{(G_0 \cdot V^\alpha)^{\frac{1}{d}} - 1} \left( 1 - \frac{1}{G_0 \cdot V^\alpha} \right) \quad (4)$$

Where  $d$  is the number of dynode stages, and  $\delta$  is the secondary emission ratio for each dynode, which represents the current amplification that occurs after the electrons impinge into each respective dynode. When taking into account this factor, we obtained the following corrected expressions for the gain and the number of photoelectrons [3]:

$$G = \frac{G_{meas}}{1 + F}, \quad N_{phe} = \frac{Q}{e \cdot G} \quad (5)$$

Where  $G_{meas}$  is the measured gain value and  $G$  is the corrected gain value.

We adjusted the laser intensity values to each PMT, HV value, and measurement type because gain only depends on the HV and not on the laser intensity.

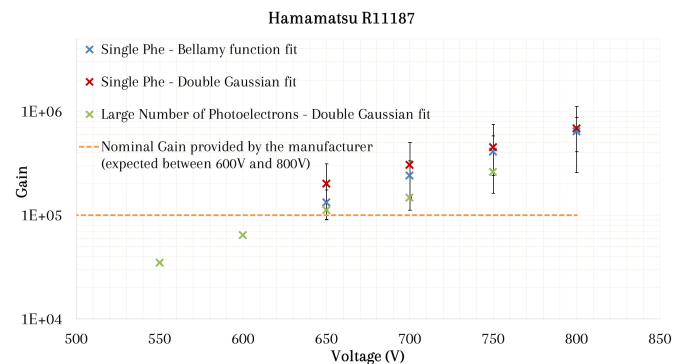


Figure 6: Representation of the Gain-HV relation obtained through all different kinds of data analysis methods for the Hamamatsu R11187. Numeric values for the fitting parameters ( $G_0$  and  $\alpha$ ) for each of the methodologies can be found at Appendix B.

Figures 6 and 7 show that the obtained gain values corresponding to different types of measurements and

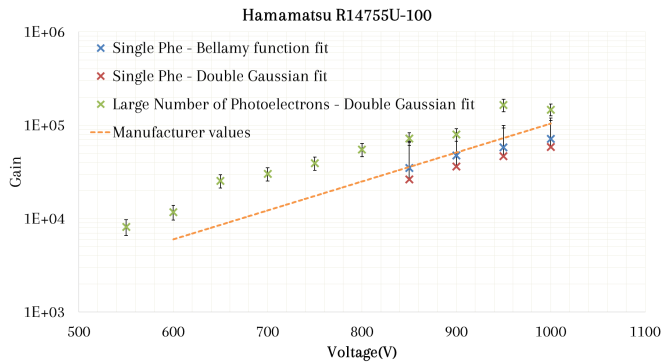


Figure 7: Representation of the Gain-HV relation obtained through all different kinds of data analysis methods for the Hamamatsu R14755U-100. Numeric values for the fitting parameters ( $G_0$  and  $\alpha$ ) for each of the methodologies can be found at Appendix B.

data analysis techniques for both PMTs concur with the information provided by the manufacturer [7, 8] with a maximum discrepancy of a factor 2, which taking into account the represented error bars and the manufacturing process expected variations, is an acceptable difference.

Therefore, we consider all applied data analysis methodologies valid for the characterization of the Hamamatsu R11187 and the Hamamatsu R14755U-100 at the respective voltage ranges studied (optimal working ranges). As expected, the Hamamatsu R11187 has a much higher gain than the Hamamatsu R14755U-100.

### III. CONCLUSIONS

Going back to the gain and time resolution requirements stipulated in this work’s introduction, we can assess whether the PMTs studied are fitted for the LHC Run 5.

Regarding time resolution, we have obtained fairly similar values for both PMTs working under the same laser intensity conditions. Given the minor differences between

these values, we can not conclude that one of the PMT models has a higher viability of implementation than the other one. However, since the values obtained for both PMTs are below the established bound ( $\sigma_t = 20ps$ ), we can state that both PMTs’ time resolution values meet the agreed requirements for implementation.

For gain results, we have clearly seen that, as expected, the Hamamatsu R14755U-100 has a much lower gain than the Hamamatsu R11187. This makes the Hamamatsu R14755U-100 more fitted for the innermost zone of the calorimeter in terms of gain, provided that a lower gain will reduce the aging of the detector. However, the Hamamatsu R14755U-100 will need to operate on the lower end of its optimal voltage range in order to fulfill the established gain requirements (staying between  $10^3$  and  $4 \cdot 10^3$ ).

In closing, we have managed to design different methodologies of measurement and data analysis, which have been validated by the agreement between the gain values provided by the manufacturer and the ones obtained at the laboratory. These methodologies can be extrapolated to any other PMT characterization case in the future. This implies that, in the case that additional test beam data containing the number of photoelectrons at which the PMTs will operate at LHCb Run 5 is received, making new measurements and analyzing results will be significantly faster and more efficient.

### Acknowledgements

I would like to express my deepest gratitude towards my advisor Eduardo Picatoste, for his guidance, patience, and opportunity to take part in such a fascinating project, as well as towards Albert Espinya and Oscar de la Torre, for their help with the implementation of the data analysis programs. I would also like to thank David Gascón for welcoming me into his research group. Finally, my sincerest thank you to my family and friends, for their unconditional support throughout this project.

- 
- [1] Calorimeter system at the large hadron collider beauty experiment. <https://lhcb-outreach.web.cern.ch/detector/calorimeter-system/>. Accessed: 2023-10-01.
  - [2] E. Bellamy, G. Bellettini, J. Budagov, F. Cervelli, I. Chirikov-Zorin, M. Incagli, D. Lucchesi, C. Pagliarone, S. Tokar, and F. Zetti. Absolute calibration and monitoring of a spectrometric channel using a photomultiplier. *Nuclear Instruments and Methods in Physics Research Section A: Accelerators, Spectrometers, Detectors and Associated Equipment*, 339(3):468–476, 1994.
  - [3] N. Bouhemaïd, M. Crouau, A. Gil-Botella, S. González de la Hoz, P. Grenier, G. Montarou, G. S. Muanza, S. Poirot, and F. Vazeille. Characterization of the Hamamatsu 10-stages R5900 photomultipliers at Clermont for the TILE calorimeter. 4 1997.
  - [4] T. L. Collaboration. The lhcb detector at the lhcb. *Journal of Instrumentation*, 3(08):S08005, aug 2008.
  - [5] J.-F. G. G. V. Fukun and T. H. Frischa. Signal processing for pico-second resolution timing measurements. *arXiv preprint arXiv:0810.5590*, 2008.
  - [6] K. Hamamatsu Photonics. Photomultiplier tubes: Basics and applications. *Edition 3a*, 310, 2007.
  - [7] Hamamatsu Photonics K.K. *Photomultiplier tube R11187*, 8 2009.
  - [8] Hamamatsu Photonics K.K. *Metal package Photomultiplier tube R14755U-100*, 2020.
  - [9] M. Salomoni. The Upgrade II of the LHCb Calorimeter. 2021.

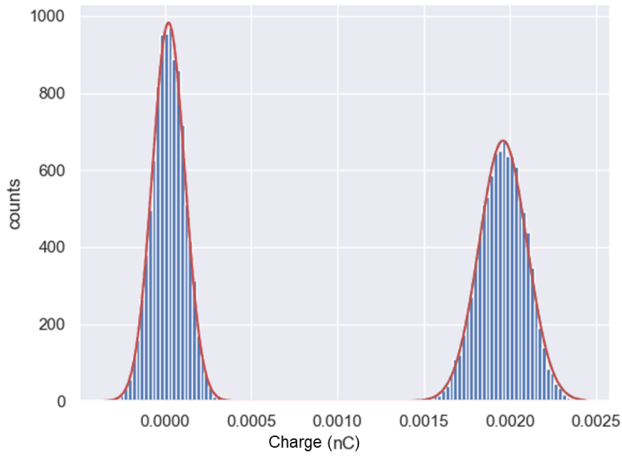
**Appendix A: Double Gaussian fit**


Figure 8: Charge(nC) histogram of a Large Number of Photoelectrons measurement for the Hamamatsu R14755U-100 PMT at  $HV = 550V$  fitted by a Double Gaussian.

**Appendix B:  $G_0$  and  $\alpha$  values**

Adjusting the  $G = G_0 \cdot V^\alpha$  fit to the data represented in Figures 6 and 7, the value of the  $G_0$  and  $\alpha$  parameters has been obtained for each of the data analysis methodologies:

	<b>R14755U-100</b>		<b>R11187</b>	
	$G_0$	$\alpha$	$G_0$	$\alpha$
<b>1 Phe (Bellamy)</b>	$5.64 \cdot 10^{-9}$	4.37	$5.83 \cdot 10^{-17}$	7.60
<b>1 Phe (Gaussian)</b>	$1.58 \cdot 10^{-10}$	4.86	$5.71 \cdot 10^{-12}$	5.88
<b>N Phe (Gaussian)</b>	$3.26 \cdot 10^{-10}$	4.90	$2.22 \cdot 10^{-13}$	6.28
<b>Manufacturer</b>	$9.92 \cdot 10^{-11}$	4.96	-	-

Table I: Comparison table for  $G_0$  and  $\alpha$  parameter values.

The apparent discrepancy between the values obtained for each of the data analysis methods for the Hamamatsu R11187 comes from the exponential relation between the gain and the supply voltage: small variations in the gain values can result in big changes in the fitting parameters.